Journal of Computational Mathematics, Vol.20, No.4, 2002, 391–412.

NUMERICAL STUDIES OF 2D FREE SURFACE WAVES WITH FIXED BOTTOM*[1)]

Ping-wen Zhang
(*School of Mathematics Sciences, Peking University, Beijing, 100871, China*)

Xiao-ming Zheng
(*Department of AMS, State University of New York, Stony Brook, NY 11794-3600, USA*)

Abstract

The motion of surface waves under the effect of bottom is a very interesting and challenging phenomenon in the nature. we use boundary integral method to compute and analyze this problem. In the linear analysis, the linearized equations have bounded error increase under some compatible conditions. This contributes to the cancellation of instable Kelvin-Helmholtz terms. Under the effect of bottom, the existence of equations is hard to determine, but given some limitations it proves true. These limitations are that the swing of interfaces should be small enough, and the distance between surface and bottom should be large enough. In order to maintain the stability of computation, some compatible relationship must be satisfied like that of [5]. In the numerical examples, the simulation of standing waves and breaking waves are calculated. And in the case of shallow bottom, we found that the behavior of waves are rather singular.

Key words: Fixed bottom, 2D surface wave, Boundary integral method, Linear analysis, Energy analysis.

1. Introduction

It is well known that the solution to the Dirichlet and Neumann problems for Laplace's equation may be expressed in terms of boundary integrals of source or dipole distributions. In this method, the boundary is always labelled as Lagrange markers. Numerical methods with Lagrange markers were attempted for vortex sheets long ago by Rosenhead. Such Methods for more general fluid interfaces were first proposed by Birkhoff [6]. The first successful boundary intergral method (BIM) was developed by Longuet-Higgins and Cokelet [21], who calculated plunging breakers. BIM for the exact, time-dependent equations have been developed and used in many other works, including Vinje, Brevig [33], Baker, Meiron, Orszag [2], Pullin [26], New, Mclver, Peregrine [24], Dold [10], Schwartz, Fenton [29]. Yeung [35] reviewed these early works. Methods of boundary integral type have been used even for the ill-posed cases of fluid interface motion, including vortex sheets and Reyleigh-Taylor instability (Moore [22], Krasny [20], Kerr [19], Tryggvason [32], Shelley [30]), a regularization or filtering of high wave numbers is necessary for numerical stability.

Flows such as those generated by surface waves over bottom topography or due to a solid body in motion underneath an interface require Neumann boundary conditions at the solid boundaries in addition to the free-surface conditions. Since the fluid can not penetrate a solid boundary, the normal fluid velocity at the body must equal the normal body velocity. The bottom boundary and interface are assumed to be 2π-periodic in the horizontal direction. Using the complex variables, we parametrize the free surface and solid boundary by $z_F(\alpha, t)$ and $z_B(\alpha, t)$ respectively. The bottom is assumed stationary. We take α as the Lagrange coordinate; i.e., dz_F/dt is the velocity of the lower fluid at the surface. The dipole moment and

* Received November 29, 1999.
[1)] Supported by the Special Funds for Major State Basic Research Projects of China G1999032804 and the National Natural Science Foundation of China.

source moment can be determined from the potential and boundaries by resolving two linear integral equations. It is important that the integral equations are two Fredholm equations of the second kind, they can be solved by simple iterative procedures. Verchota [34] and Kenig [17][18] proved the existence of solution in the bounded domain with Lipscitz boundary. Beale, Hou and Lowengrub [4] proved that the Fredholm equation has solution in $H^s, s \geq 0$ in half plane with smooth boundary. But it is hard to extend this result to system. We use an iterative sequence to construct a solution and at the same time look for the sufficient conditions to guarantee the existence of this solution. We find it is suffice to force the distance between surface and bottom large enough and the perturbation of surface is small enough. And the later condition is the same to the idea that the free surface is sufficiently close to equilibrium, which is well-known as the condition of well-posedness of free surface according to W.Craig [8] and H. Yosihara [36]. Although they are not satisfactory conditions, it is compatible with the computation and we expect the proof of existence of more relaxed conditions, or even the removement of such limitations.

The stability of numerical methods is closely related to the question studied in section 2 of the well-posedness of arbitrary linearizations, since the numerical error can be expected to satisfy the linear equations to first approximations. Beale, Hou and Lowengrub [5] presented a convergence proof of a boundary integral for water waves with or without surface tension. Following a framework developed in [4] for linearized motion perturbed about an arbitrary smooth solution at the continuous level, they found that very delicate balances among terms with singular integrals and derivatives must be preserved at the discrete level in order to maintain numerical stability. They also realized that suitable numerical filtering is necessary at certain places to prevent the discretization from introducing new instabilities in the high modes. This filtering depends on the choices for approximating spatial derivatives and quadrature rules for singular integrals. Besides filtering, Hou and Zhang [16] discovered a new stablizing method which compensates the unstable terms, the new method can be expanded to 3-D water waves. In order to illustrate the necessity of filtering, we develop a group of numerical experiments to show the differences that filtering brings with bottom. While the comparison under the case without bottom was shown in [5]. When the bottom is considered, it doesn't bring any singularity to the velocity, which make the numerical analysis and computation comparatively easy to work on, provided realizing the solvablity of the linearized Fredholm equations (see (29), (30)).

The advantage of using alternating trapezoidal quadrature is that the approximation is spectrally accurate. Sidi and Israeli [31] analyzed the spectral accuracy of a midpoint rule approximation for a periodic singular integrate. They realized that the alternating quadrature rule applied to singular integrals gives spectral accuracy. Shelley [30] used this scheme in the context of studying the cortex sheet singularity by vortex methods. By using the spectral accuracy of the alternating trapezoidal rule, Hou, Lowengrub and Krasny [14] simplifed the proof of the convergence of the point vortex method for vortex sheets.

The rest of the paper is organized as follows: The following in Section 1 is devoted to describe the boundary integral reformulation introduced by Beale, Hou and Lowengrub [5] and their ideas to remove numerical instabilities. In Section 2, we present our linearize analysis in continuous level. The numerical analysis is given in Section 3. Finally, in Section 5, some numerical examples are included to demonstrate the robustness of the method. Numerical simulation of shallow and deep water proceed to a time where it approximates the singularity. The method remains stable even in the full nonlinear regime of motion.

1.1. Analytical Formulas

We consider the 2D incompressible, inviscid and irrotational fluid bounded by upper free boundary and lower fixed bottom. Based on the potential theory and partial differential equations, we can regard the interface as dipole layer, and bottom as source layer with potential flow, thus there exist potential function and stream function.

Assuming there is a source with strength m at $z(e)$, then at any place z except $z(e)$ the potential function and stream function are:

$$\phi_s = \frac{m}{2\pi}\ln r, \qquad \psi_s = \frac{m}{2\pi}\theta,$$

where $r = |z - z(e)|$, $\quad \theta = \arctan\frac{y-y(e)}{x-x(e)}$.

Alternatively assuming there is a dipole with strength μ_F at $z(e)$, then at any place z except $z(e)$, the potential function and stream function are:

$$\phi_d = \frac{\mu_F}{2\pi}\frac{\partial \ln r}{\partial n(e)}, \quad \psi_d = \frac{\mu_F}{2\pi}\frac{\partial \theta}{\partial n(e)}, \tag{1}$$

where $n(e)$ is the unit vector of dipole from sink to source.

Integrating along the source layer, we get the complex potential at z:

$$\Phi_s(z) = \int \{\phi_s(e) + i\psi_s(e)\}ds(e) = \frac{1}{2\pi}\int m(e)\ln(z - z(e))ds(e). \tag{2}$$

Let $\sigma(e) = m(e)\cdot s_e(e)$, then

$$\Phi_s(z) = \frac{1}{2\pi}\int \sigma(e)\ln(z - z(e))de. \tag{3}$$

Similarly we have the complex potential generated by dipole layer:

$$\Phi_d(z) = \int \{\phi_d(e) + i\psi_d(e)\}ds(e) = \frac{1}{2\pi i}\int \frac{\mu_F(e)z_e(e)}{z - z(e)}de. \tag{4}$$

We denote the surface $z_F(e)$, and bottom $z_B(e)$, Thus the general complex potential is:

$$\Phi(z) = \frac{1}{2\pi i}\int \frac{\mu_F(e)z_{F_e}(e)}{z - z_F(e)}de + \frac{1}{2\pi}\int \sigma(e)\ln(z - z_B(e))de. \tag{5}$$

Because $\sigma(e) = [\mu_B(e)]_e$, integrating the second term by parts, we obtain

$$\Phi(z) = \frac{1}{2\pi i}\int \frac{\mu_F(e)z_{F_e}(e)}{z - z_F(e)}de + \frac{1}{2\pi}\int \frac{\mu_B(e)z_{B_e}(e)}{z - z_B(e)}de. \tag{6}$$

Set $\Phi(z) = \phi(z) + i\psi(z)$, it follows from the Plemelj formula of complex variables the value of ϕ on the surface is:

$$\phi(\alpha) = \frac{1}{2}\mu_F(\alpha) + Re\left[\frac{1}{2\pi i}\int \frac{\mu_F(\alpha')z_{F_\alpha}(\alpha')}{z_F(\alpha) - z_F(\alpha')}d\alpha' + \frac{1}{2\pi}\int \frac{\mu_B(\alpha')z_{B_\alpha}(\alpha')}{z_F(\alpha) - z_B(\alpha')}d\alpha'\right]. \tag{7}$$

By differentiating above equation with respect to α, there results a Fredholm equation for γ,

$$\phi_\alpha = \frac{1}{2}\gamma(\alpha) + Re\left[\frac{z_{F_\alpha}(\alpha)}{2\pi i}\int \frac{\gamma(\alpha')}{z_F(\alpha) - z_F(\alpha')}d\alpha' + \frac{z_{F_\alpha}(\alpha)}{2\pi}\int \frac{\sigma(\alpha')}{z_F(\alpha) - z_B(\alpha')}d\alpha'\right]. \tag{8}$$

Differentiating the complex potential with respect to z, we get the complex velocity ω:

$$\omega(z) = \frac{d\Phi}{dz} = \frac{1}{2\pi i}\int \frac{\gamma(e)}{z - z_F(e)}de + \frac{1}{2\pi}\int \frac{\sigma(e)}{z - z_B(e)}de. \tag{9}$$

By Plemelj formula, we obtain the complex velocity on the surface:

$$\omega(\alpha) = \frac{\gamma(\alpha)}{2z_{F_\alpha}(\alpha)} + \frac{1}{2\pi i}\int \frac{\gamma(\alpha')}{z_F(\alpha) - z_F(\alpha')}d\alpha' + \frac{1}{2\pi}\int \frac{\sigma(\alpha')}{z_F(\alpha) - z_B(\alpha')}d\alpha'. \tag{10}$$

Along the bottom, the stream function ψ must be a constant (zero for convenience). Using Plemelj formula on the bottom, we obtain:

$$\frac{\mu_B(\alpha)}{2} = Im\left[\frac{1}{2\pi i}\int \frac{\mu_F(\alpha')z_{F_\alpha}(\alpha')}{z_B(\alpha) - z_F(\alpha')}d\alpha' + \frac{1}{2\pi}\int \frac{\mu_B(\alpha')z_{B_\alpha}(\alpha')}{z_B(\alpha) - z_B(\alpha')}d\alpha'\right]. \tag{11}$$

By differentiating (11) with respect to α, there results a Fredholm equation for σ:

$$\begin{aligned}\frac{\sigma(\alpha)}{2} = Im\Bigg[&\frac{z_{B_\alpha}(\alpha)}{2\pi i}\int \gamma(\alpha')\frac{1}{z_B(\alpha) - z_F(\alpha')}d\alpha' \\ &+\frac{z_{B_\alpha}(\alpha)}{2\pi}\int \sigma(\alpha')\frac{1}{z_B(\alpha) - z_B(\alpha')}d\alpha'\Bigg].\end{aligned} \tag{12}$$

Since α is a Lagrange coordinate, the velocity of the interface is that of the fluid below, and we obtain an evolution equation for the interface:

$$\frac{\partial z}{\partial t}(\alpha,t)=\omega^*(\alpha,t), \tag{13}$$

where the asterisk denotes the complex conjugate. For the evolution of $\phi(\alpha,t)$, we use Bernoulli equation. If we neglect surface tension, the pressure is zero at the interface. Thus, Bernoulli equation in the Lagrange frame is

$$\phi_t-\frac{1}{2}|\omega|^2+gy=0. \tag{14}$$

To summarize, we obtain the entire evolution system consisting of (8), (10), (12), (13) and (14).

1.2. Numerical Formulas

From now on, with $z(\alpha,t)=\alpha+s(\alpha,t)$ (**Note**: in this paper, we would always denote $z_F(\alpha,t)$ or $z_B(\alpha,t)$ as $z(\alpha,t)$ when we want to endow them the same properties), we assume that $s(\alpha,t)$ and $\phi(\alpha,t)$ are periodic in α with period 2π. With

$$\frac{1}{2}\cot\frac{z}{2}=\sum_{k=-\infty}^{+\infty}\frac{1}{z+2k\pi},\quad z\neq 2k\pi, k\in\mathcal{Z},$$

we obtain the complex potential under periodic condition:

$$\Phi(z)=\frac{1}{4\pi i}\int_{-\pi}^{\pi}\mu_F(\alpha')z_{F_\alpha}\cot\frac{z-z_F(\alpha')}{2}d\alpha'+\frac{1}{4\pi}\int_{-\pi}^{\pi}\mu_B(\alpha')z_{B_\alpha}\cot\frac{z-z_B(\alpha')}{2}d\alpha',$$

and other equations under period 2π:

$$\begin{aligned}\phi_\alpha &= \frac{1}{2}\gamma(\alpha)+Re\left[\frac{z_{F_\alpha}(\alpha)}{4\pi i}\int_{-\pi}^{\pi}\gamma(\alpha')\cot\frac{z_F(\alpha)-z_F(\alpha')}{2}d\alpha'\right.\\ &\quad\left.+\frac{z_{F_\alpha}(\alpha)}{4\pi}\int_{-\pi}^{\pi}\sigma(\alpha')\cot\frac{z_F(\alpha)-z_B(\alpha')}{2}d\alpha'\right],\end{aligned} \tag{15}$$

$$\begin{aligned}\frac{\sigma(\alpha)}{2} &= Im\left[\frac{z_{B_\alpha}(\alpha)}{4\pi i}\int_{-\pi}^{\pi}\gamma(\alpha')\cot\frac{z_B(\alpha)-z_F(\alpha')}{2}d\alpha'\right.\\ &\quad\left.+\frac{z_{B_\alpha}(\alpha)}{4\pi}\int_{-\pi}^{\pi}\sigma(\alpha')\cot\frac{z_B(\alpha)-z_B(\alpha')}{2}d\alpha'\right],\end{aligned} \tag{16}$$

$$\begin{aligned}\omega(\alpha) &= \frac{\gamma(\alpha)}{2z_{F_\alpha}}(\alpha)+\frac{1}{4\pi i}\int_{-\pi}^{\pi}\gamma(\alpha')\cot\frac{z_F(\alpha)-z_F(\alpha')}{2}d\alpha'\\ &\quad+\frac{1}{4\pi}\int_{-\pi}^{\pi}\sigma(\alpha')\cot\frac{z_F(\alpha)-z_B(\alpha')}{2}d\alpha',\end{aligned} \tag{17}$$

We use the same discrete scheme as that of [5], and the following is a simple repeat: Dividing $[-\pi,\pi]$ uniformly into N parts, set $\alpha_j=jh, h=\frac{2\pi}{N}, j=-\frac{N}{2}+1,\cdots,\frac{N}{2}$. Introduce discrete operator D_h, whose Fourier symbol is

$$(\hat{D}_h f)_k=ik\rho(kh)\hat{f}_k,\ k=-\frac{N}{2}+1,\cdots,\frac{N}{2}. \tag{18}$$

That D_h is of order 'r' refers to the fact that ρ satisfies

$$|1-\rho(kh)|\le C(kh)^r.$$

For the second-order centered difference operator,we have:

$$\rho_2(kh) = \frac{\sin(kh)}{kh};$$

for the fourth-order centered difference scheme,

$$\rho_4(kh) = \frac{8\sin(kh) - \sin(2kh)}{6kh};$$

and for the cubic spline approximation,

$$\rho_c(kh) = \left[\frac{\sin(kh)}{kh}\frac{3}{2+\cos(kh)}\right].$$

If D_h is spectral derivative, it satisfies(i) $\rho(-x) = \rho(x)$, $\rho(x) > 0$; (ii) $\rho \in C^2$, $\rho(\pi) = 0$; (iii) $\rho(x)$=1 when$|x| \le \lambda\pi$, where $0 < \lambda < 1$. For example, when

$$\rho(kh) \ = \ exp(-10(2|k|h)^{25}) \ , \quad |k| \le N/2,$$

$(\hat{D}_h)_k = ik\rho(kh)$ is a 25-order accurate approximation to the derivative operator.

The meaning of filtering is as follows: let z_j be an approximation to $z(\alpha_j)$, $s_j = z_j - \alpha_j$ will be periodic. We define z_j^p as $\alpha_j + s_j^p$, where

$$\hat{s}_k^p = \rho(kh) \cdot \hat{s}_k \ . \tag{19}$$

It is clear that z^p is an rth-order approximation to z if ρ corresponds to the rth-order derivative operator.

In order to approximate the singular integral, given the discrete functions $z_j \approx z(\alpha_j)$ and $\gamma_j \approx \gamma(\alpha_j)$, we use the alternating trapezoidal rule, with filtering in z_F as above:

$$\int_{-\pi}^{\pi} \gamma(\alpha') \cot \frac{z_F(\alpha_i) - z_F(\alpha')}{2} d\alpha' \approx \sum_{\substack{j=-N/2+1 \\ (j-i) odd}}^{N/2} \gamma_j \cot\left(\frac{z_{F_i}^p - z_{F_j}^p}{2}\right) 2h. \tag{20}$$

Dealing with other integrals with the same rule, we obtain the following numerical formula:

$$\begin{aligned} \frac{dz_i^*}{dt} &= \frac{\gamma_i}{2(D_h z)_i} + \frac{1}{4\pi i} \sum_{\substack{j=-N/2+1 \\ (j-i) odd}}^{N/2} \gamma_j \cot\left(\frac{z_{F_i}^p - z_{F_j}^p}{2}\right) 2h \\ &\quad + \frac{1}{4\pi} \sum_{\substack{j=-N/2+1 \\ (j-i) odd}}^{N/2} \sigma_j \cot\left(\frac{z_{F_i} - z_{B_j}}{2}\right) 2h = u_i - iv_i \ , \end{aligned} \tag{21}$$

$$\frac{d\phi_i}{dt} = \frac{1}{2}(u_i^2 + v_i^2) - gy_i, \tag{22}$$

$$\begin{aligned} D_h\phi_i &= \frac{\gamma_i}{2} + Re\left[\frac{D_h z_{F_i}}{4\pi i} \sum_{\substack{j=-N/2+1 \\ (j-i) odd}}^{N/2} \gamma_j \cot\left(\frac{z_{F_i}^p - z_{F_j}^p}{2}\right) 2h \right. \\ &\quad \left. \frac{D_h z_{F_i}}{4\pi} \sum_{\substack{j=-N/2+1 \\ (j-i) odd}}^{N/2} \sigma_j \cot\left(\frac{z_{F_i} - z_{B_j}}{2}\right) 2h\right], \end{aligned} \tag{23}$$

$$\begin{aligned} \frac{\sigma_i}{2} &= Im\left[\frac{D_h z_{B_i}}{4\pi i} \sum_{\substack{j=-N/2+1 \\ (j-i) odd}}^{N/2} \gamma_j \cot\left(\frac{z_{B_i} - z_{F_j}}{2}\right) 2h \right. \\ &\quad \left. \frac{D_h z_{B_i}}{4\pi} \sum_{\substack{j=-N/2+1 \\ (j-i) odd}}^{N/2} \sigma_j \cot\left(\frac{z_{B_i} - z_{B_j}}{2}\right) 2h\right]. \end{aligned} \tag{24}$$

2. Linear Analysis

2.1. Existence and Uniqueness of Fredholm Equations

Definition 2.1. *We define the integral operators*

$$\begin{aligned} K_1\gamma(\alpha) &= Re\left\{\frac{1}{2\pi i}\int_{\alpha'}\frac{\gamma(\alpha')z_{F_\alpha}(\alpha')}{z_F(\alpha)-z_F(\alpha')}d\alpha'\right\}, \\ K_2\sigma(\alpha) &= Re\left\{\frac{1}{2\pi}\int_{\alpha'}\frac{\sigma(\alpha')z_{F_\alpha}(\alpha)}{z_F(\alpha)-z_B(\alpha')}d\alpha'\right\}, \\ K_3\gamma(\alpha) &= -Im\left\{\frac{1}{2\pi i}\int_{\alpha'}\frac{\gamma(\alpha')z_{B_\alpha}(\alpha)}{z_B(\alpha)-z_F(\alpha')}d\alpha'\right\}, \\ K_4\sigma(\alpha) &= Im\left\{\frac{1}{2\pi}\int_{\alpha'}\frac{\sigma(\alpha')z_{B_\alpha}(\alpha')}{z_B(\alpha)-z_B(\alpha')}d\alpha'\right\}. \end{aligned}$$

Definition 2.2. $(*)$ *condition:*

(1) $z_F(\alpha)-\alpha\in H^m(\mathbb{R}), z_B(\alpha)-\alpha\in H^m(\mathbb{R}), m\geq 3,$

(2) $0 \leq s \leq m-2,$

(3) $\exists c_b>0, h_B>0,\ s.t. |z_F(\alpha)-z_B(\alpha')|^2 > c_b^2(\alpha-\alpha')^2+h_B^2, \forall\alpha,\alpha'\in\mathbb{R}.$

Lemma 2.1. *Under the* $(*)$ *condition,*

$$\pm\frac{1}{2}I+K_{1,4} \quad and \quad \pm\frac{1}{2}I+K_{1,4}^*$$

has bounded inverse on $H^s(\mathbb{R})$.

Proof. See [4] Theorem 3.

The Fredholm equations (15), (16) composed by γ,σ is

$$\left(\frac{1}{2}I-K_1^*\right)\gamma = \phi_\alpha - K_2\sigma, \tag{25}$$

$$\left(\frac{1}{2}I+K_4^*\right)\sigma = -K_3\gamma, \tag{26}$$

$\forall(\gamma_0,\sigma_0)\in H^s(\mathbb{R})\times H^s(\mathbb{R})$, processing iteration:

$$\begin{aligned} (\frac{1}{2}I-K_1^*)\gamma_{n+1} &= \phi_\alpha-K_2\sigma_n, \\ (\frac{1}{2}I+K_4^*)\sigma_{n+1} &= -K_3\gamma_n, \\ & n=0,1,2,\cdots \end{aligned}$$

when $n\geq 2$,

$$\begin{aligned} (\frac{1}{2}I-K_1^*)(\gamma_{n+1}-\gamma_n) &= -K_2(\sigma_n-\sigma_{n-1}) \\ &= (-K_2)(\frac{1}{2}I+K_4^*)^{-1}(-K_3)(\gamma_{n-1}-\gamma_{n-2}). \end{aligned}$$

Let $\epsilon_n=\gamma_n-\gamma_{n-1}$, then

$$\epsilon_{n+1}=(\frac{1}{2}I-K_1^*)^{-1}\cdot K_2\cdot(\frac{1}{2}I+K_4^*)^{-1}\cdot K_3\cdot\epsilon_{n-1}.$$

if we define

$$T=(\frac{1}{2}I-K_1^*)^{-1}\cdot K_2\cdot(\frac{1}{2}I+K_4^*)^{-1}\cdot K_3,$$

it follows

$$\epsilon_{2k+1}=T^k\epsilon_1,\ \epsilon_{2k+2}=T^k\epsilon_2,\ k=0,1,2,\cdots,$$

In order that the iterative sequence converge, it suffices to have $\epsilon_{2k+1} \to 0$ and $\epsilon_{2k+2} \to 0$ which can be satisfied if $\|T\| < 1$ (in some normed space).

First we consider the space $L^2 \times L^2$: $(\gamma, \sigma) \in L^2(\mathbb{R}) \times L^2(\mathbb{R})$, and we try to find the conditions to ensure $\|T\|_{L^2} < 1$.

In order that $\|T\|_{L^2} < 1$ it suffices to have

$$\begin{aligned} \|(\frac{1}{2}I - K_1^*)^{-1}\|_{L^2} \cdot \|K_2\|_{L^2} &< 1 \\ \|(\frac{1}{2}I + K_4^*)^{-1}\|_{L^2} \cdot \|K_3\|_{L^2} &< 1 \end{aligned} \tag{27}$$

Assumption 2.1. *$y = F(x)$ on $\partial\Omega$ and assume $\exists C_F$, s.t.*

$$|F''(x)| < C_F \quad , \forall x \tag{28}$$

and $0 < \delta < 1$, s.t.

$$\begin{aligned} & 1 + \delta > && |z_F(\alpha')| && > 1 - \delta \\ i.e. \quad & 1 + \delta > && |\{x_\alpha(\alpha') \ , \ y_\alpha(\alpha')\}| && > 1 - \delta \end{aligned}$$

Theorem 2.1. *Under $(*)$ condition and Assumption2.1, there exist $C_{1F}^* > 0, h_{1B}^* > 0$, when $C_F < C_{1F}^*$, $h_B > h_{1B}^*$, γ, σ equations have unique solution in $H^s(\mathbb{R}) \times H^s(\mathbb{R})$.*

2.2. Linear Analysis

Lemma 2.2. *Assuming*

$$\begin{aligned} K_5 f(\alpha) &= Re\left[\frac{1}{2\pi}\int \frac{f(\alpha')z_{B_\alpha}(\alpha')}{z_F(\alpha) - z_B(\alpha')}d\alpha'\right], \\ K_6 f(\alpha) &= Im\left[\frac{1}{2\pi i}\int \frac{f(\alpha')z_{F_\alpha}(\alpha')}{z_B(\alpha) - z_F(\alpha')}d\alpha'\right], \end{aligned}$$

and K_1 as above, then we have

$$\begin{aligned} (K_1 f)^{\cdot}(\alpha) &= (K_1 \dot{f})(\alpha) + Re\left[\frac{1}{2\pi i}\int f_\alpha(\alpha')\frac{\dot{z}_F(\alpha) - \dot{z}_F(\alpha')}{z_F(\alpha) - z_F(\alpha')}d\alpha'\right], \\ (K_5 f)^{\cdot}(\alpha) &= (K_5 \dot{f})(\alpha) + Re\left[\frac{1}{2\pi}\int f_\alpha(\alpha')\frac{\dot{z}_F(\alpha)}{z_F(\alpha) - z_B(\alpha')}d\alpha'\right], \\ (K_6 f)^{\cdot}(\alpha) &= (K_6 \dot{f})(\alpha) - Im\left[\frac{1}{2\pi i}\int f_\alpha(\alpha')\frac{\dot{z}_F(\alpha')}{z_B(\alpha) - z_F(\alpha')}d\alpha'\right]. \end{aligned}$$

Proof. The same as Lemma 2.4 in [4].

Lemma 2.3. *When $0 \le s \le m-2$, denoting z_F or z_B as z, then the Cauchy integral*

$$\mathcal{K}\rho(\alpha) = \frac{1}{2\pi i}\int \frac{\rho(\alpha')z_\alpha(\alpha')}{z(\alpha) - z(\alpha')}d\alpha'$$

defines a bounded operator on H^s. And $\mathcal{K}_1\rho(\alpha) = \mathcal{K}\rho(\alpha) - \frac{1}{2i}H\rho(\alpha)$ is a smooth operator from H^0 to H^{m-2}.

Proof. See Lemma 2.2 in [4].

Corollary 2.1. *$K_1 f = Re(\mathcal{K})$ is a smooth operator.*

Proof. $K_1 f = Re(\mathcal{K}) = Re(\mathcal{K} - \frac{1}{2i}Hf) = Re(\mathcal{K}_1)$.

Lemma 2.4.
$$F(\dot\sigma) = \frac{1}{2\pi}\int_{\alpha'\in\mathbb{R}} \frac{\dot\sigma}{z_F(\alpha)-z_B(\alpha')}d\alpha' = A_{-\infty}(\dot\sigma)$$
$$(i.e.\ \ H^0 \overset{b.d.d.}{\longrightarrow} H^{m-2})$$

Proof. From $(*)$ condition (3), we have
$$|z_F(\alpha)-z_B(\alpha')|^2 \geq c_b((\alpha-\alpha')^2+h_B^2),$$
then
$$\begin{aligned}\|F(\dot\sigma)\|_{H_0}^2 &\leq \frac{1}{2\pi^2}\int_{\alpha'\in\mathbb{R}}\frac{|\dot\sigma(\alpha')|^2}{c_b^2[(\alpha-\alpha')^2+h_B^2]}d\alpha\int_{\alpha\in\mathbb{R}}d\alpha \\ &< c_3\|\dot\sigma\|_{H_0}^2\end{aligned}$$
Using the same method as that applied to $D^\gamma F(\dot\sigma)$ ($|\gamma|\leq m-2$), the conclusion is obtained.

Similarly, K_2, K_3, K_5, K_6 are also smooth operators.

From the definition of Definition 2.1 and Lemma 2.3, the Fredholm equations can be reduced to
$$\begin{aligned}\phi &= K_1\mu_F+\frac{1}{2}\mu_F+K_5\mu_B, \\ \frac{\mu_B}{2} &= K_6\mu_F+K_4\mu_B.\end{aligned}$$
Employing relative results in [4] and above Lemma, we obtain the linearized equation for $\dot\mu_F$ and $\dot\mu_B$:
$$\begin{aligned}\dot\phi &= \frac{1}{2}\dot\mu_F+K_1\dot\mu_F+Re[(\omega_0+\omega_1)\dot z_F]+K_5\dot\mu_B-Re\left(\frac{1}{2i}\frac{\gamma}{z_{F_\alpha}}H\dot z_F\right), \\ &\quad +A_{-\infty}(\dot z_F) \qquad (29)\\ \dot\mu_B &= 2K_6\dot\mu_F+2K_4\dot\mu_B+A_{-\infty}(\dot z_F), \qquad (30)\end{aligned}$$
where
$$\begin{aligned}\omega_0(\alpha) &= \frac{1}{2\pi i}\int\frac{\gamma(\alpha')}{z_F(\alpha)-z_F(\alpha')}d\alpha', \\ \omega_1(\alpha) &= \frac{1}{2\pi}\int\frac{\sigma(\alpha')}{z_F(\alpha)-z_B(\alpha')}d\alpha'.\end{aligned}$$
This is also a Fredholm system similar to that in former section. We conclude
$$\begin{aligned}|\dot\mu_F|_s &\leq c(|\dot z_F|_s+|\dot\phi|_s), \\ |\dot\mu_B|_s &\leq c(|\dot z_F|_s+|\dot\phi|_s), \\ 0 &\leq s \leq m-2. \qquad (31)\end{aligned}$$
Differentiating (29) with respect to α, we get
$$\begin{aligned}\dot\phi_\alpha &= \frac{1}{2}\dot\gamma+D_\alpha(K_1\dot\mu_F)+Re[(\omega_0+\omega_1)\dot z_{F_\alpha}]+D_\alpha K_5\dot\mu_B \qquad (32)\\ &\quad -D_\alpha Im\left(\frac{\gamma}{2z_{F_\alpha}}H\dot z_F\right)+A_0(\dot z_F). \qquad (33)\end{aligned}$$
Using (31), because K_1, K_5 are smooth operators, there results
$$\dot\gamma = 2\dot\phi_\alpha-2Re[(\omega_0+\omega_1)\dot z_{F_\alpha}]+D_\alpha Im\frac{\gamma}{z_\alpha}H\dot z_F+A_0(\dot z_F)+A_{-\infty}(\dot\phi). \qquad (34)$$
Defining $\rho=\gamma/z_{F_\alpha}$, recalling the linearized equation for $\dot\omega$ from [4] and our equation for ω (10), we obtain
$$\begin{aligned}\dot\omega &= \frac{1}{2}(I-iH)\dot\rho+A_{-\infty}(\dot\rho)+A_0(\dot z_F)+\frac{1}{2\pi}\int\frac{\dot\sigma(\alpha')}{z_F(\alpha)-z_B(\alpha')}d\alpha' \\ &\quad +\frac{1}{2\pi}\int\left(\frac{\sigma}{z_{B_\alpha}}\right)_\alpha(\alpha')\frac{\dot z_F(\alpha)}{z_F(\alpha)-z_B(\alpha')}d\alpha', \qquad (35)\end{aligned}$$

Similar to Lemma2.5, we have

$$\frac{1}{2\pi}\int\left(\frac{\sigma}{z_{B_\alpha}}\right)_\alpha(\alpha')\frac{\dot z_F(\alpha)}{z_F(\alpha)-z_B(\alpha')}d\alpha' = A_{-\infty}(\dot z_{F_i}), \tag{36}$$

which follows

$$\dot\omega = \frac{1}{2}(I-iH)\dot\rho + A_0(\dot z_F) + A_{-\infty}(\dot\phi), \tag{37}$$

where $\dot\rho = \dot\gamma/z_{F_\alpha} - \gamma z_{F_\alpha}/z_{F_\alpha}^2$. Substituting $\dot\gamma$ with (34), we find

$$\dot\omega = \frac{1}{2}(I-iH)D_\alpha[\dot\phi - Re(\omega\dot z_F)] + A_0(\dot z_F) + A_{-\infty}(\dot\phi), \tag{38}$$

Then the remaining proof is the same as [4], we have our conclusion:

Theorem 2.2. *Under* $(*)$ *condition and Assumption 2.1, there exist* $C_{1F}^*>0$, $h_{1B}^*>0$, *when* $C_F<C_{1F}^*$, $h_B>h_{1B}^*$, *and furthermore*

$$(u_t,v_t)\cdot\vec n - (0,-g)\cdot\vec n \ge c_0 > 0 \tag{39}$$

holds at every point of the surface. Here (u,v) *is the Lagrange velocity,* $\vec n$ *is the outer unit normal,* c_0 *is constant. Then the solution of the linearized equations satisfy*

$$|\dot z_F(t)|_s^2 + |\dot\phi(t)|_s^2 \le B_s(t)(|\dot z_F(0)|_{s+1/2}^2 + |\dot\phi(0)|_{s+1/2}^2)$$

3. Numerical Analysis

Definition 3.1.

$$T^* = sup\{t|t\le T, \|\dot z\|_{l^2}, \|\dot\phi\|_{l^2} \le h^{5/2}, \|\dot\gamma\|_{l^2}\le h^{3/2}\} \tag{40}$$

Definition 3.2.

$$K_N = \{k\in\mathcal N, -N/2+1 \ \le\ k\ \le\ N/2, N is\ even\}$$

Error estimates will be given in terms of the discrete space is $l^2(K_N)$: a discrete function z is said to be in $l^2(K_N)$ iff

$$\|z\|_{l^2}^2 = \sum_{j=-N/2+1}^{N/2}|z_j|^2h<\infty. \tag{41}$$

Note. We will use l^2 to stand for $l^2(K_N)$ for convenience in the following proof.

We have the same conclusion as [5]:

$$\begin{aligned}\|\dot z\|_\infty &\le h^2,\ t\le T^*;\\ \|\dot\gamma\|_\infty &\le h^2,\ t\le T^*;\\ \|D_h\dot z\|_\infty &\le 2\pi h,\ t\le T^*;\\ \|\dot\zeta^{NL}\|_{l^2} &\le C\|\dot z\|_{l^2},\ t\le T^*.\end{aligned} \tag{42}$$

Definition 3.3. *We define discrete integral operators*

$$\begin{aligned}K_{1h}\gamma_i &= Re\left\{\frac{1}{2\pi i}\sum_{j\in\mathcal Z}^{(j-i)odd}\frac{\gamma_j D_h z_{F_j}}{z_{F_i}^p - z_{F_j}^p}d\alpha'\right\},\\ K_{2h}\sigma_i &= Re\left\{\frac{1}{2\pi}\sum_{j\in\mathcal Z}^{(j-i)odd}\frac{\sigma_j D_h z_{F_i}}{z_{F_i} - z_{B_j}}d\alpha'\right\},\\ K_{3h}\gamma_i &= -Im\left\{\frac{1}{2\pi i}\sum_{j\in\mathcal Z}^{(j-i)odd}\frac{\gamma_j D_h z_{B_i}}{z_{B_i} - z_{F_j}}d\alpha'\right\},\\ K_{4h}\sigma_i &= Im\left\{\frac{1}{2\pi}\sum_{j\in\mathcal Z}^{(j-i)odd}\frac{\sigma_j D_h z_{B_j}}{z_{B_i} - z_{B_j}}d\alpha'\right\}.\end{aligned}$$

First we give the convergence proof of discrete formula, which is the base of energy analysis.

3.1. Existence of Solution for Discrete Fredholm Equations

Under the discrete condition, we introduce a lemma in [5]:

Lemma 3.1. *Assume $z_F(\cdot,t)$, $z_F(\cdot,t) \in C^3$, $z_{F_\alpha}, z_{B_\alpha} \neq 0$, then there exist constants h_0 and $C > 0$, s.t. $\forall h$ when $0 < h \le h_0$,*

$$\|(\frac{1}{2}I \pm K^*_{(1,4)h})^{-1}\| \le C, \tag{43}$$

$$\|(\frac{1}{2}I \pm K_{(1,4)h})^{-1}\| \le C. \tag{44}$$

Define

$$T_h = (\frac{1}{2}I - K^*_{h1})^{-1} \cdot K_{2h} \cdot (\frac{1}{2}I + K^*_{h4})^{-1} \cdot K_{3h}$$

Theorem 3.1. *Under $(*)$ condition, if C_F is small enough, h_B is large enough, and h small enough, then $(I \pm T_h)$ is inversible on $l^2 \times l^2$.*

3.2. Stability

From [5] we introduce some notations:

$$E_i = \frac{1}{2\pi i}\sum_{(j-i)odd}\frac{\gamma_j}{z^p_{F_i} - z^p_{F_j}}2h\ ,\quad \zeta_i = \frac{\gamma_i}{D_h z_{F_i}},\quad Q_i = \frac{D_h z_{F_i}}{2\pi i}\sum_{(j-i)odd}\frac{\gamma_j}{z^p_{F_i} - z^p_{F_j}}2h,$$

and their errors:

$$\dot{E}_j + \frac{1}{2}\dot{\zeta}_j = \frac{1}{2z_{F_\alpha}(\alpha_j)}(I - iH_h)\left(\dot{\gamma}_j - \frac{\gamma(\alpha_j)}{2z_{F_\alpha}(\alpha_j)}D_h\dot{z}_{F_j}\right) + A_0(\dot{z}_{F_j}) + A_{-1}(\dot{\gamma}_j) + R_h(\dot{\gamma}_j), \tag{45}$$

$$\begin{aligned}\dot{Q}_i \;=\;& D_h\dot{z}_{F_i}\omega_0(\alpha_i) + \frac{D_h z_F(\alpha_i)}{2\pi i}\sum_{(j-i)odd}\frac{\dot{\gamma}_j}{z_F(\alpha_i)^p - z_F(\alpha_j)^p}2h \\ & -\frac{\gamma(\alpha_i)}{2iz_{F_\alpha}(\alpha_i)}H_hD_h(\dot{z}_{F_i}) + A_0(\dot{z}_{F_i}).\end{aligned} \tag{46}$$

From the definition of K_{1h}, we get

$$Re(\dot{Q}_i) = K^*_{1h}(\dot{\gamma}) + Re\left\{D_h\dot{z}_{F_i}\omega_0(\alpha_i) - \frac{\gamma(\alpha_i)}{2iz_{F_\alpha}(\alpha_i)}H_hD_h(\dot{z}_{F_i})\right\} + A_0(\dot{z}_{F_i}). \tag{47}$$

Because the bottom z_B is fixed , naturally we set $\dot{z}_B = 0$ in the following analysis.
We define

$$G_i = \frac{1}{2\pi}\sum_{(j-i)odd}\frac{\sigma_j}{z_{F_i} - z_{B_j}}2h, \tag{48}$$

and direct calculations show that the linear part $\dot{G}^L_i$ is given by

$$\dot{G}^L_i = \frac{1}{2\pi}\sum_{(j-i)odd}\left(\frac{\dot{\sigma}_j}{z_F(\alpha_i) - z_B(\alpha_j)} - \frac{\sigma(\alpha_j)\dot{z}_{F_i}}{[z_F(\alpha_i) - z_B(\alpha_j)]^2}\right)2h, \tag{49}$$

and nonlinear part $\dot{G}^{NL}_i$ is given by

$$\begin{aligned}\dot{G}^{NL}_i \;=\;& \frac{1}{2\pi}\sum_{(j-i)odd}\frac{\sigma(\alpha_j)\dot{z}^2_{F_i}}{[z_F(\alpha_i) - z_B(\alpha_j)][z_F(\alpha_i) - z_B(\alpha_j) + \dot{z}_{F_i}]}2h \\ & -\frac{1}{2\pi}\sum_{(j-i)odd}\frac{\dot{\sigma}_j\dot{z}_{F_i}}{[z_F(\alpha_i) - z_B(\alpha_j)][z_F(\alpha_i) - z_B(\alpha_j) + \dot{z}_{F_i}]}2h.\end{aligned} \tag{50}$$

To estimate the linear part of $\dot{G}_i$, we need to introduce a lemma:

Lemma 3.2.

$$\frac{1}{2\pi}\sum_{(j-i)odd}\frac{\dot{\sigma}_j}{z_F(\alpha_i)-z_B(\alpha_j)}2h = A_{-m}(\dot{\sigma}) \tag{51}$$

Analogously, K_{2h}, K_{3h} are also operators of kind A_{-m}, and

$$\frac{1}{2\pi}\sum_{(j-i)odd}\frac{\sigma(\alpha_j)\dot{z}_{F_i}}{[z_F(\alpha_i)-z_B(\alpha_j)]^2}2h = A_0(\dot{z}_{F_i}) \tag{52}$$

We use the same method as [5] to estimate the two terms in $\dot{G}^{NL}$:

$$\begin{aligned}
\frac{1}{2\pi}\sum_{(j-i)odd}\frac{\sigma(\alpha_j)\dot{z}_{F_i}^2}{[z_F(\alpha_i)-z_B(\alpha_j)][z_F(\alpha_i)-z_B(\alpha_j)+\dot{z}_{F_i}]}2h &= A_0(\dot{z}_{F_i}),\\
\frac{1}{2\pi}\sum_{(j-i)odd}\frac{\dot{\sigma}_j\dot{z}_{F_i}}{[z_F(\alpha_i)-z_B(\alpha_j)][z_F(\alpha_i)-z_B(\alpha_j)+\dot{z}_{F_i}]}2h &= A_0(\dot{z}_{F_i}),
\end{aligned} \tag{53}$$

then we have

$$\dot{G}_i = A_{-m}(\dot{\sigma}) + A_0(\dot{z}_{F_i}). \tag{54}$$

Defining

$$P_i = \frac{D_h z_{F_i}}{2\pi}\sum_{(j-i)odd}\frac{\sigma_j}{z_F(\alpha_i)-z_B(\alpha_j)}2h, \tag{55}$$

we get

$$\begin{aligned}
\dot{P}_i &= \frac{D_h\dot{z}_{F_i}}{2\pi}\sum_{(j-i)odd}\frac{\sigma_j}{z_F(\alpha_i)-z_B(\alpha_j)}2h + D_h z_F(\alpha_i)\dot{G}_i\\
&= \frac{D_h\dot{z}_{F_i}}{2\pi}\left(\int\frac{\sigma(\alpha')}{z_F(\alpha)-z_B(\alpha')}d\alpha' + O(h^r)\right) + D_h z_F(\alpha_i)\dot{G}_i,
\end{aligned}$$

recalling the decomposition of $\dot{G}_i$, it follows

$$\dot{P}_i = D_h\dot{z}_{F_i}\omega_1 + D_h z_F(\alpha_i)\frac{1}{2\pi}\sum_{(j-i)odd}\frac{\dot{\sigma}_j}{z_F(\alpha_i)-z_B(\alpha_j)}2h + A_0(\dot{z}_{F_I}). \tag{56}$$

From the definition of K_{2h}, we have

$$Re(\dot{P}_i) = Re(D_h\dot{z}_{F_i}\omega_1) + K_{2h}(\dot{\sigma}_i) + A_0(\dot{z}_{F_i}). \tag{57}$$

Defining

$$X_i = \frac{D_h z_{B_i}}{2\pi}\sum_{(j-i)odd}\frac{\dot{\gamma}_j}{z_B(\alpha_i)-z_F(\alpha_j)}2h, \tag{58}$$

using the similar methods as above, we get

$$\begin{aligned}
\dot{X}_i^L &= \frac{D_h z_{B_i}}{2\pi i}\sum_{(j-i)odd}\left(\frac{\dot{\gamma}_j}{z_B(\alpha_i)-z_F(\alpha_j)} - \frac{\gamma(\alpha_j)\dot{z}_{F_j}}{[z_B(\alpha_i)-z_F(\alpha_j)]^2}\right)2h\\
&= A_{-1}(\dot{\gamma}) + A_0(\dot{z}_F),
\end{aligned} \tag{59}$$

and

$$\begin{aligned}
\dot{X}_i^{NL} &= \frac{D_h z_{B_i}}{2\pi i}\sum_{(j-i)odd}\frac{\gamma(\alpha_j)\dot{z}_{F_j}^2}{[z_B(\alpha_i)-z_B(\alpha_j)][z_B(\alpha_i)-z_F(\alpha_j)-\dot{z}_{F_j}]}2h\\
&\quad+\frac{1}{2\pi}\sum_{(j-i)odd}\frac{\dot{\gamma}_j\dot{z}_{F_i}}{[z_B(\alpha_i)-z_F(\alpha_j)][z_B(\alpha_i)-z_F(\alpha_j)-\dot{z}_{F_j}]}2h,\\
\dot{X}_i^{NL} &= A_0(\dot{z}_{F_i}).
\end{aligned} \tag{60}$$

Then

$$\dot{X}_i = A_{-1}(\dot{\gamma}) + A_0(\dot{z}_{F_i}), \tag{61}$$

and from the definition of K_{3h}, we obtain

$$Im(\dot{X}_i) = -K_{3h}(\dot{\gamma}) + A_0(\dot{z}_{F_i}). \tag{62}$$

We define

$$Y_i = \frac{D_h z_{B_i}}{2\pi} \sum_{(j-i)odd} \frac{\sigma_j}{z_B(\alpha_i) - z_B(\alpha_j)} 2h, \tag{63}$$

then

$$\dot{Y}_i = \frac{D_h z_{B_i}}{2\pi} \sum_{(j-i)odd} \frac{\dot{\sigma}_j}{z_B(\alpha_i) - z_B(\alpha_j)} 2h, \tag{64}$$

from the definition of K_{4h},

$$Im(\dot{Y}_i) = -K^*_{4h}(\dot{\sigma}_i). \tag{65}$$

3.3. Energy Analysis

Based on the above results, we get:

$$\begin{cases} \dot{\omega}_i &= \dot{E}_i + \dot{G}_i + \frac{1}{2}\dot{\zeta}_i + O(h^r) \\ D_h\dot{\phi}_i &= \frac{\dot{\gamma}_i}{2} + Re(\dot{Q}_i + \dot{P}_i) + O(h^r) \\ \dot{\sigma}_i &= 2Im[\dot{X}_i + \dot{Y}_i] + O(h^r) \end{cases}$$

From $\dot{X}$ and $\dot{Y}$, we know

$$\dot{\sigma}_i = -2K^*_{4h}(\dot{\sigma}_i) - 2K_{3h}(\dot{\gamma}_i) + A_0(\dot{z}_{F_i}) + O(h^r) \tag{66}$$

and from the theory of operator (see [5]),

$$\frac{1}{2}I + K^*_{4h}(\bullet_i)$$

has bounded inverse on l_2 , then we have

$$\dot{\sigma}_i = -(\frac{1}{2}I + K^*_{4h})^{-1}K_{3h}(\dot{\gamma}_i) + A_0(\dot{z}_{F_i}) + O(h^r). \tag{67}$$

From the expression of $\dot{Q}_i$ and $\dot{P}_i$

$$\begin{aligned} D_h\dot{\phi}_i &= \frac{\dot{\gamma}_i}{2} - K^*_{1h}(\dot{\gamma}_i) + K_{2h}(\dot{\sigma}_i) + Re\,[D_h((\omega_0+\omega_1)\dot{z}_{F_i})] \\ &\quad + A_0(\dot{z}_{F_i}) - Re\left[\frac{\gamma(\alpha_i)}{2iz_{F_\alpha}(\alpha_i)} H_h D_h \dot{z}_{F_i}\right], \end{aligned}$$

substituting the expression of $\dot{\gamma}_i$ into above formula, we get:

$$\begin{aligned} (\frac{1}{2}I - K^*_{1h})\dot{\gamma}_i &= D_h\dot{\phi}_i + K_{2h}(\frac{1}{2}I + K^*_{4h})^{-1}K_{3h}(\dot{\gamma}_i) \\ &\quad - Re[\omega_2(\alpha_i)D_h\dot{z}_{F_i}] + D_hH_hIm\left[\frac{\gamma(\alpha_i)}{2z_{F_\alpha}(\alpha_i)}\dot{z}_i\right] \\ &\quad + A_0(\dot{z}_{F_i}) + O(h^r), \end{aligned} \tag{68}$$

where

$$\omega_2(\alpha_i) = \omega_0(\alpha_i) + \omega_1(\alpha_i).$$

Owing to the inversibility of $\frac{1}{2}I - K^*_{1h}$, we get

$$\begin{aligned} (I - T_h)\dot{\gamma}_i &= (\frac{1}{2}I - K^*_{1h})^{-1}\Big\{D_h\dot{\phi}_i - Re[\omega_2(\alpha_i)D_h\dot{z}_{F_i}] \\ &\quad + D_hH_hIm\left[\frac{\gamma(\alpha_i)}{2z_{F_\alpha}(\alpha_i)}\dot{z}_i\right]\Big\} + A_0(\dot{z}_{F_i}) + O(h^r), \end{aligned} \tag{69}$$

Because $(I - T_h)^{-1}$ is bounded, when the above formula is operated by operator of A_{-1} type, the terms including derivative are all transformed into bounded terms. Then

$$A_{-1}(\dot{\gamma}_i) = A_0(\dot{z}_{F_i}) + A_0(\dot{\phi}_i)$$

We introduce Lemma 1 of [5]:

Lemma 3.3. *Assume $f(\cdot) \in C^3$, $\omega \in l^2$, then*

$$D_h(f(\alpha_i)\omega_i) = f(\alpha_i)D_h(\omega_i) + \omega_i^q f_\alpha(\alpha_i) + A_{-1}(\omega_i)$$

where $\hat{\omega}_k^q = \hat{\omega}_k q(kh)$, $q(x) = \frac{d}{dx}(\rho(x)x)$.

Set

$$\dot{W} = \left\{ \dot{\phi}_i - Re[\omega_2(\alpha_i)\dot{z}_{F_i}] + H_h Im \left[\frac{\gamma(\alpha_i)}{2z_{F_\alpha}(\alpha_i)} \dot{z}_i \right] \right\}, \tag{70}$$

as to the second terms in (70), use the above lemma,

$$D_h\dot{W} = \left\{ D_h\dot{\phi}_i - Re[\omega_2(\alpha_i)D_h\dot{z}_{F_i}] + D_h H_h Im \left[\frac{\gamma(\alpha_i)}{2z_{F_\alpha}(\alpha_i)} \dot{z}_i \right] \right\} + A_0(\dot{z}_{F_i}) + O(h^r).$$

We already have

$$\begin{aligned} \dot{\gamma}_i &= (I - T_h)^{-1}(\frac{1}{2}I - K_{1h}^*)^{-1} \Big\{ D_h\dot{\phi}_i - Re[\omega_2(\alpha_i)D_h\dot{z}_{F_i}] \\ &\quad + D_h H_h Im \left[\frac{\gamma(\alpha_i)}{2z_{F_\alpha}(\alpha_i)} \dot{z}_i \right] \Big\} + A_0(\dot{z}_{F_i}) + O(h^r), \end{aligned} \tag{71}$$

and substitute it into following formula:

$$\dot{\sigma}_i = -(\frac{1}{2}I + K_{4h}^*)^{-1} K_{3h}(\dot{\gamma}_i) + A_0(\dot{z}_{F_i}) + O(h^r), \tag{72}$$

and get:

$$\begin{aligned} K_{2h}\dot{\sigma}_i &= -K_{2h}(\frac{1}{2}I + K_{4h}^*)^{-1} K_{3h}(I - T_h)^{-1}(\frac{1}{2}I - K_{1h}^*)^{-1} \Big\{ D_h\dot{\phi}_i - Re[\omega_2(\alpha_i)D_h\dot{z}_{F_i}] \\ &\quad + D_h H_h Im \left[\frac{\gamma(\alpha_i)}{2z_{F_\alpha}(\alpha_i)} \dot{z}_i \right] \Big\} + A_0(\dot{z}_{F_i}) + O(h^r). \end{aligned} \tag{73}$$

Because K_{2h}, K_{3h} is of type A_{-m} and the terms in the right parenthese only have 1-order derivatives, thus the above formula can be reduced to

$$K_{2h}\dot{\sigma}_i = A_0(\dot{z}_i) + A_0(\dot{\phi}) + O(h^r) \tag{74}$$

we obtain the estimate for $\dot{\gamma}$:

$$\begin{aligned} \dot{\gamma}_i &= \Big\{ 2D_h\dot{\phi}_i - 2Re[\omega_2(\alpha_i)D_h\dot{z}_{F_i}] + D_h H_h Im \left[\frac{\gamma(\alpha_i)}{z_{F_\alpha}(\alpha_i)} \dot{z}_i \right] \\ &\quad + A_0(\dot{z}_{F_i}) + A_0(\dot{\phi}_i) + O(h^r) \Big\}. \end{aligned} \tag{75}$$

In the stability analysis, we have obtained $\dot{\omega}_i$, $\dot{E}_i$, $\dot{G}_i$ and $\dot{\zeta}_i$, now we substitute them into $d\dot{z}_i^*/dt$:

$$\begin{aligned} \frac{d\dot{z}_i^*}{dt} &= \frac{1}{2z_\alpha(\alpha_i)}(I - iH_h) \left[\dot{\gamma}_i - \frac{\gamma_i}{z_\alpha(\alpha_i)} D_h\dot{z}_i \right] + A_0(\dot{z}_F) \\ &\quad + A_{-1}(\dot{\gamma}_i) + A_{-1}(\dot{\sigma}) + R_h(\dot{\gamma}_i) + O(h^r). \end{aligned} \tag{76}$$

From [5] we know:

$$R_h(\dot{\gamma}) = A_0(\dot{z}_i) + A_0(\dot{\phi}) + O(h^r), \tag{77}$$

then

$$\begin{aligned} \frac{d\dot{z}_i^*}{dt} &= \frac{1}{2z_\alpha(\alpha_i)}(I - iH_h) \left[\dot{\gamma}_i - \frac{\gamma_i}{z_\alpha(\alpha_i)} D_h\dot{z}_i \right] \\ &\quad + A_0(\dot{z}_i) + A_0(\dot{\phi}) + O(h^r). \end{aligned} \tag{78}$$

Now applying $(I - iH_h)$ to both sides of (75), similar to [5], we obtain

$$\begin{aligned} (I - iH_h)\dot{\gamma}_i &= (I - iH_h) \Big[2D_h\dot{\phi}_i - 2Re(\omega_2(\alpha_i)D_h\dot{z}_{F_i}) \\ &\quad + iIm \left(\frac{\gamma(\alpha_i)}{z_\alpha(\alpha_i)} D_h(\dot{z}_{F_i}) \right) \Big] + A_0(\dot{z}_{F_i}) + A_0(\dot{\phi}_i) + O(h^r). \end{aligned} \tag{79}$$

Substituting the above two terms into (76), we get

$$\frac{d\dot{z}_i^*}{dt} = \frac{1}{2z_\alpha(\alpha_i)}(I - iH_h)D_h[\dot{\phi}_i - Re(\omega(\alpha_i)\dot{z}_{F_i})] + A_0(\dot{z}_{F_i}) + A_0(\dot{\phi}_i) + O(h^r) \tag{80}$$

where

$$\omega(\alpha_i) = \omega_2(\alpha_i) + \frac{\gamma(\alpha_i)}{2z_\alpha(\alpha_i)}.$$

Then the remaining analysis is utterly the same as [5]. We state the convergence theorem for the numerical method without surface tension :

$$\|\dot{z}\|_{l^2} + \|\dot{\phi}\|_{l^2} \le B(T)h^r, \|\dot{\gamma}\|_{l^2} + \|\dot{\sigma}\|_{l^2} \le B(T)h^r, t \le T^*.$$

As for $r \ge 3$, and h small enough , we have

$$\|\dot{z}\|_{l^2} + \|\dot{\phi}\|_{l^2} \le B(T)h^{r-1}, \|\dot{\gamma}\|_{l^2} + \|\dot{\sigma}\|_{l^2} \le B(T)h^{r-2},$$

owing to the meaning of T^*, we get

$$T^* = T.$$

Theorem 3.2. *Under* $(*)$ *condition and Assumption2.1, and* $|z_F(\alpha,t)-z_F(\beta,t)| \ge c_1|\alpha-\beta|$ *when* $0 \le t \le T$ *and some* $c_1 > 0$, *and*

$$(u_t, v_t)\cdot\vec{n} - (0,-g)\cdot\vec{n} \ge c_0 > 0 \tag{81}$$

hold s at each point on the interface. Here (u,v) *is the Lagrange velocity,* $\vec{n}$ *is the outer unit normal to the interface (pointing out of the fluid region), and* c_0 *is some constant. Suppose the numerical solution* $z_F(t)$, $\phi(t)$, $\gamma(t)$, $\sigma(t)$ *of the initial value problem is computed using algorithm* (21)-(24). *Then if* D_h *is an* r*th-order derivative approximation with* $r \ge 4$, *there exist* C^*_{2F} h^*_{2B}, *and* $h_0(T)$, *s.t. when* $C_F < C^*_{2F}$, $h_B > h^*_{2B}$, $h \le h_0(T)$

$$\begin{aligned}
\|z(t) - z(\cdot,t)\|_{l^2} &\le C(T)h^r\\
\|\phi(t) - \phi(\cdot,t)\|_{l^2} &\le C(T)h^r\\
\|\gamma(t) - \gamma(\cdot,t)\|_{l^2} &\le C(T)h^r\\
\|\sigma(t) - \sigma(\cdot,t)\|_{l^2} &\le C(T)h^r
\end{aligned}$$

if D_h *is a spectral approximation as above, we have the same convergence result with* h^r *replaced by* h^m *in the right-hand sides.*

4. Numerical Examples

In this section some examples are provided to illustrate the performance of methods discussed. We calculate the standing waves and breaking wave with fixed bottom and found many interesting phenomena. We found that the bottom does affect the shape of wave, and even produce breaker in standing wave. In the computation , we found that the depth of bottom is very important. We introduce a variable "distance between surface and bottom" such as:

$$Distance = \inf_{\alpha\in[0,1]} |z_F(\alpha) - z_B(\alpha)|,$$

(the period has been normalized to unit) and when the distance is comparable to the amplitude. we regard the bottom is shallow; otherwise, deep bottom. The distance affects the converging velocity of Fredholm equations greatly, and also the shape of the wave, thus we divide this section into two subsection: deep bottom and shallow bottom. In all examples surface tension was neglected and the iteration would stop when the error between two sequential terms $< 10^{-10}$, and in most examples we use 128 points to divide the domain $[0,1]$ and choose $\Delta t = 0.0025$, except that we use 256 points and $\Delta t = 0.001$ in the computation of standing wave with bottom $y_B = -0.02$, which is a rather confusing problem.

4.1. Deep Bottom

First we give the comparison between wave with bottom and wave without bottom, when the distance is rather large. In this case, the wave is nearly periodic and the period is larger than that of wave without bottom. The initial values of standing wave are:

$$\begin{aligned}
&x_F(\alpha,0) = \alpha + 0.01\sin(2\pi\alpha), && y_F(\alpha,0) = -0.01\sin(2\pi\alpha);\\
&x_B(\alpha,0) = \alpha, && y_B(\alpha,0) = -0.3 + 0.1\sin(2\pi\alpha);\\
&\gamma(\alpha,0) = 0.01\sin(2\pi\alpha), && \alpha\in[0,1).
\end{aligned}$$

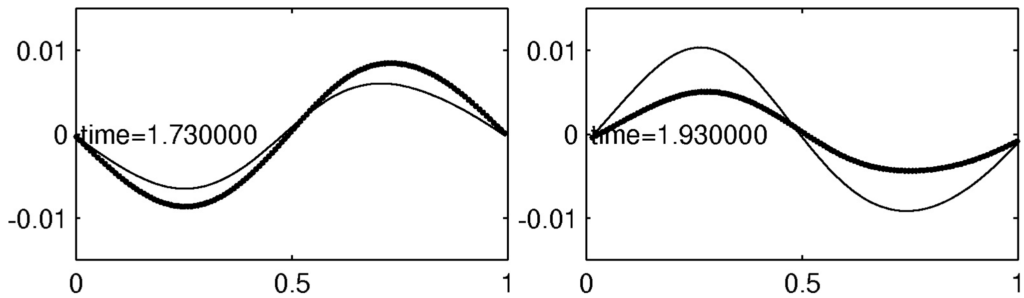

Figure 1 real line: no bottom, dot: with bottom $y_B = -0.3 + 0.1 * \sin(2\pi\alpha)$

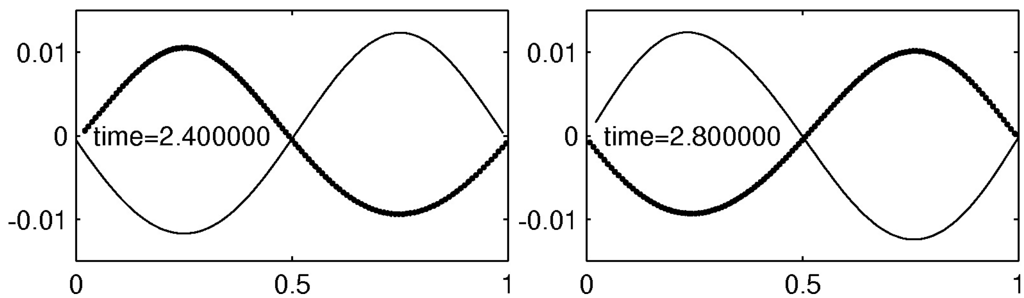

Figure 2 real line: no bottom, dot: with bottom $y_B = -0.3 + 0.1 * \sin(2\pi\alpha)$

In Figure 2, when time=2.4, two waves have departed about half wavelength.

In the computation of standing wave without bottom, if we don't use filtering, Kelvin-Helmholtz instable phenomenon would happen (see [5]). And in the computation of standing wave with fixed bottom, if we don't use filtering either, Kelvin-Helmholtz instability would happen too. For example, we set the bottom to be: $(x, -0.3 + 0.1 * \sin(2\pi x)), x \in [0, 1)$, and use 2-order centered difference to approximate the derivative. Four lines of left subfigure in Figure 3 from bottom to top are repectively the log value of spectrum of γ when time=0.6, 0.64, 0.68, 0.715. When time= 0.715, the high-frequency oscillation has been not neglectable and this is the reason why the right subfigure of γ(Figure 3) is so concussive.

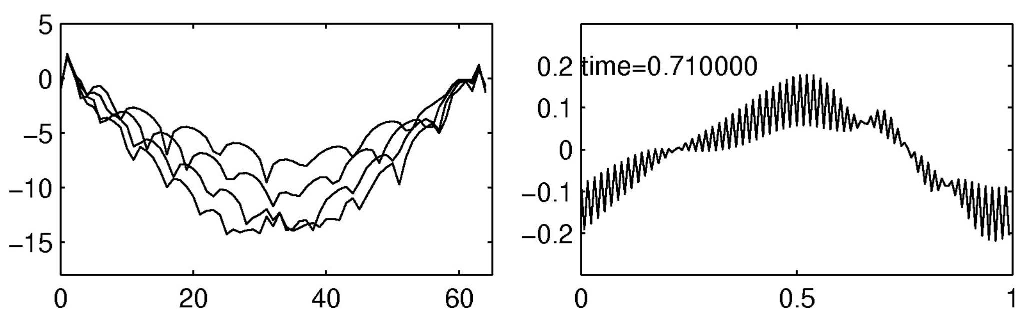

Figure 3 Second-order finite difference derivative, no filtering

4.2. Shallow Bottom

The distance affects the steration of Fredholm equations very much. For example, as to the standing wave, we set the initial value as the first example, and the bottom horizontal. Using

2-order centered difference method to approximate the derivative and Euler method to evolve in time, we gradually minish the distance between surface and bottom , and observe the iterative times:

bottom y=	-0.4	-0.2	-0.1	-0.08	-0.06	-0.04	-0.02	-0.01
iterative times	8	15	29	36	47	71	164	blow up

When bottom is y=-0.01, the distance between is already 0 which contradicts the sufficient condition of Theorem3.2. From the above table we learn that the more shallow of the bottom, the more iterative times the Fredholm equations need to converge! In fact in subsection 2.1 and subsection 3.1 we have only proved the existence of solution with large distance between surface and bottom. But we believe that there must exist solution as long as there are positive distance. We expect the proof under this more relaxed condition. Although the iteration is difficult to converge when bottom is shallow, but we can use extrapolation method to enhance the velocity. We use a fourth-order extrapolation in time to obtain a more accurate initial guess for the iterative solution for γ and σ, with a result that the iterative times decrease dramatically. For example,

bottom y=	-0.1	-0.05	-0.02
iterative times without extrapolation	28	54	164
iterative times with extrapolation	7-8	7-10	11-22

The following example computes the standing wave with bottom:

$$x_B(\alpha) = \alpha, \quad y_B(\alpha) = -0.04 + 0.01 * \sin(2\pi\alpha), \ \alpha \in [0, 1),$$

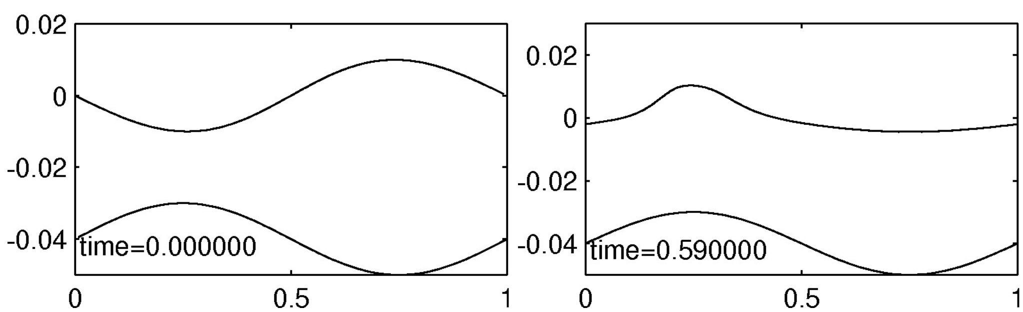

Figure 4

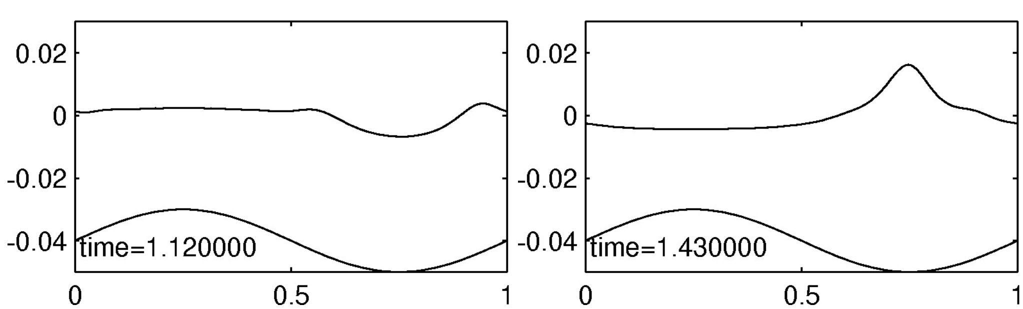

Figure 5

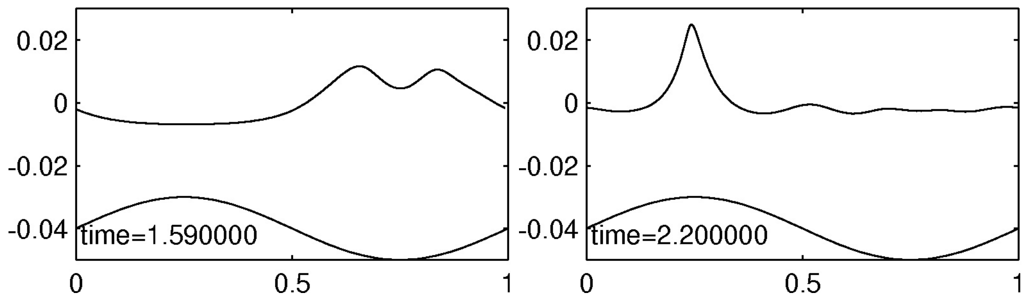

Figure 6

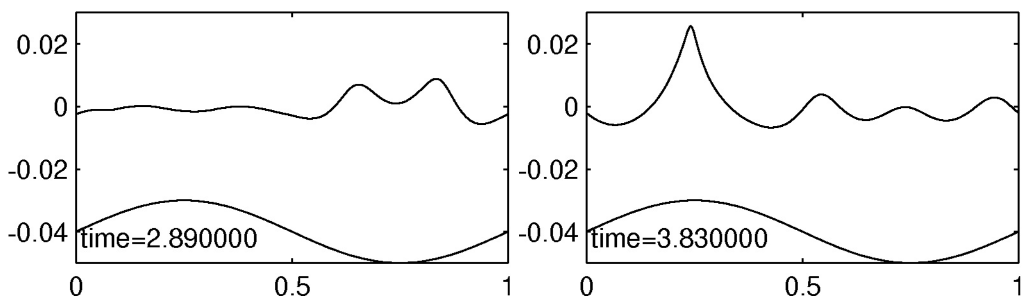

Figure 7

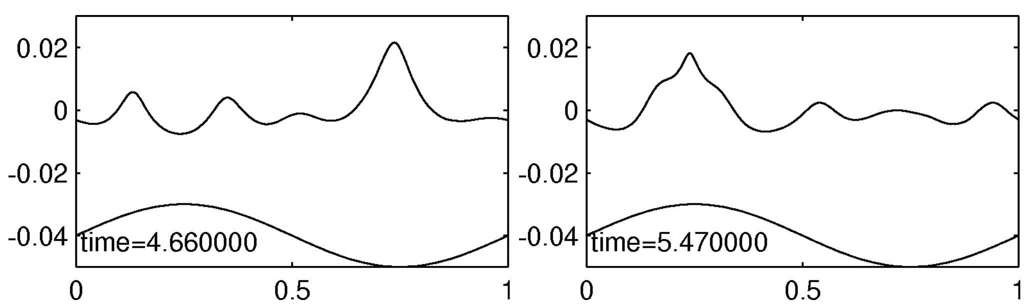

Figure 8

On $t = 0.59$ we know that the wave is largely different from the case with deep bottom; when $t = 1.43$, the crest go to the right, then breaking into two small crests with inverse direction ($t = 1.59$). Then the wave forms more high crest on the left ($t = 2.20$) and run to right again. During this process, it forms two more small crests($t = 2.89$); when the wave travel back to left, the crest is more large followed by three growing crests ($t = 3.83$). When time passing, the shape of whole wave is more singular and unexpectable.

Now we compare the above calculation with that of wave with horizontal bottom: $y_B(\alpha) = -0.04$, We illustrate some figures of this case:

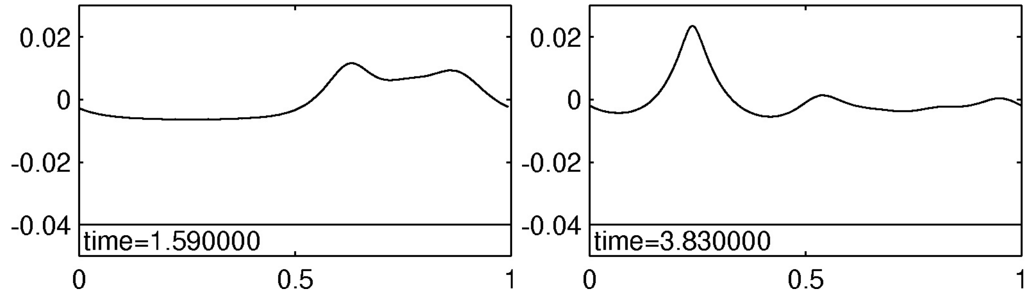

Figure 9

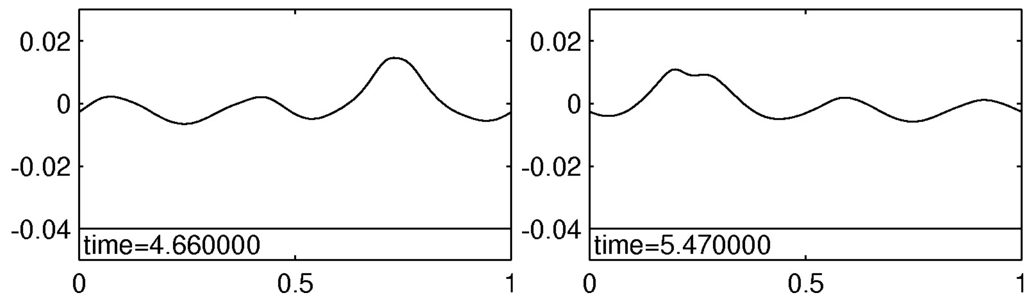

Figure 10

From the comparisons between Figure 9,10 and Figure 6,7,8 in the same time, we find that the sinine bottom generate more wave numbers than flat bottom.

Now we give a more singular computational example: wave with rising-step bottom. The bottom topography has the form $(\alpha - \sin(2\pi(\alpha - 0.5))/(2\pi), -0.04 + 0.01\sin(2\pi(\alpha - 0.5)))$.

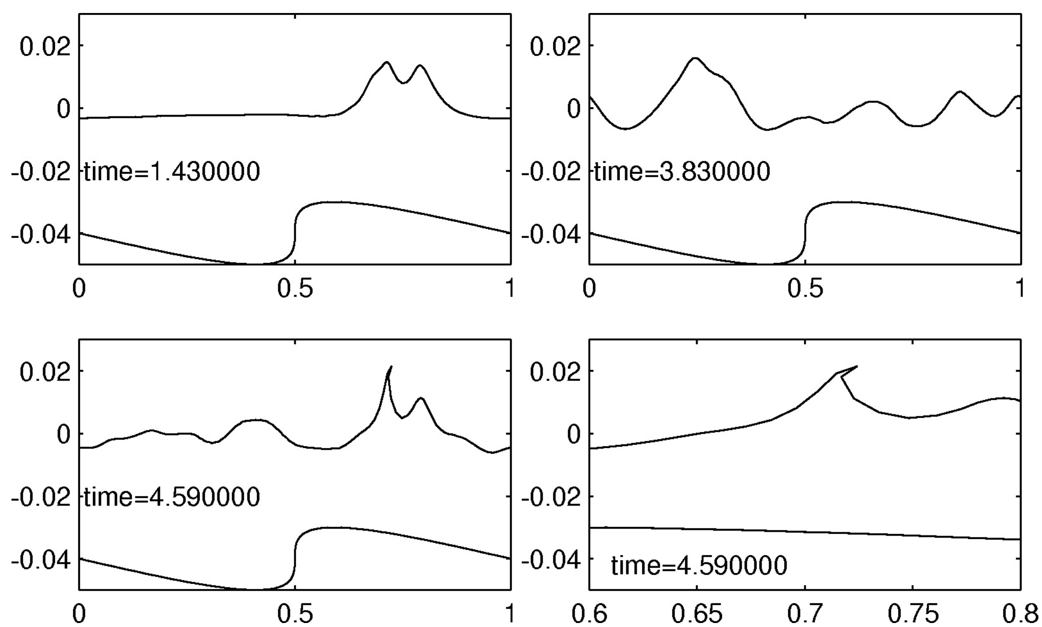

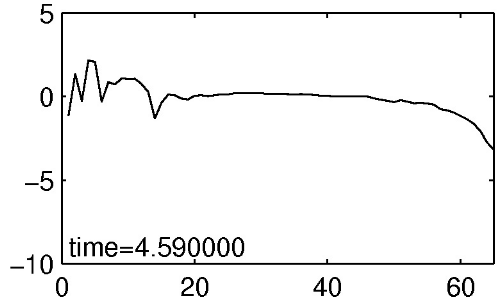

Figure 11 the fourth subfigure is the enlargement of the third subfigure, and the last figure is the log spectral plot for gamma

When $t = 4.6$, the iteration blows up and a spilling breaker formed.

When the bottom is set to be $y_B(\alpha) = -0.02$, some singular phenomenon occur. In the following figures, in order to clearly see the time evolution of the water waves, we plot two periods of waves. With N=256 and time step = 0.001, we compute up to $t = 1.215$ and then the tips comes out on the surface wave which contribute to the blow up in computation.

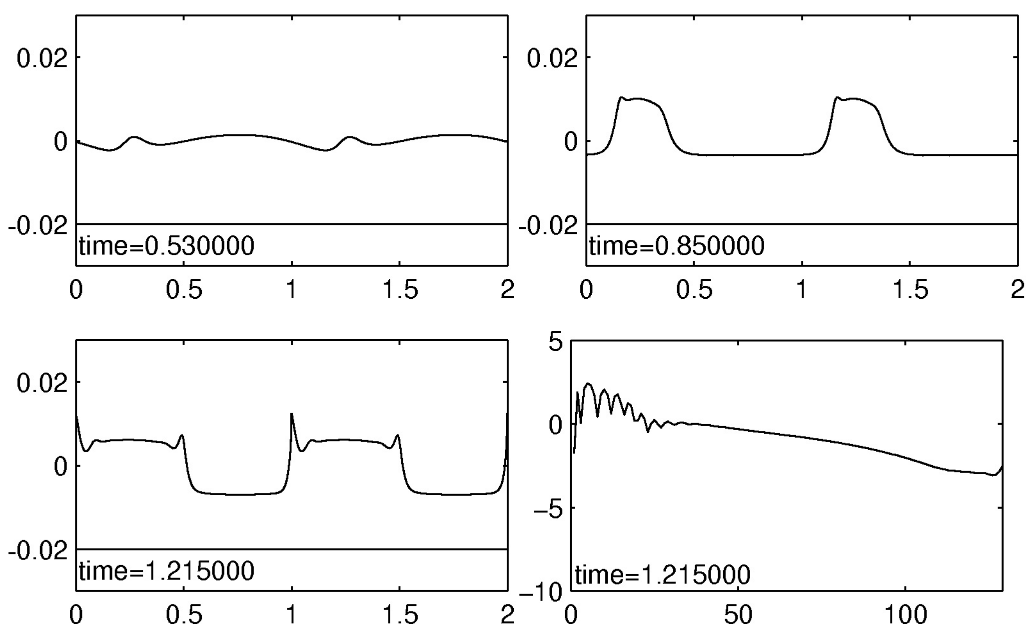

Figure 12 the last figure is the log spectral plot for gamma at $t = 1.215$

We don't know the reason to this phenomenan, but judging from the properties from above examples with shallow bottom, we guess this can be largely contributed to the nature of water waves because now the disturbance of initial wave is too large for the wave itself to hold stable.

We also compute the breaking wave above different bottom, the surface condition is always:

$$x(\alpha, 0) = \alpha,\ y(\alpha, 0) = 0.1\cos(2\pi\alpha),\ \gamma(\alpha, 0) = -1.0 + 0.1\sin(2\pi\alpha),\ \alpha \in [0, 1).$$

The time integration in this numerical example is the fourth-order explicit Adams-Bashforth method and the first four steps are Runge-Kutta method. The filtering operator is spectral stated in subsection 1.2. In the Figure 13 and 14 there are breaking waves above four bottoms, and the topic above every subgragh is the bottom equation where the horizontal coordinate is always set to be a.

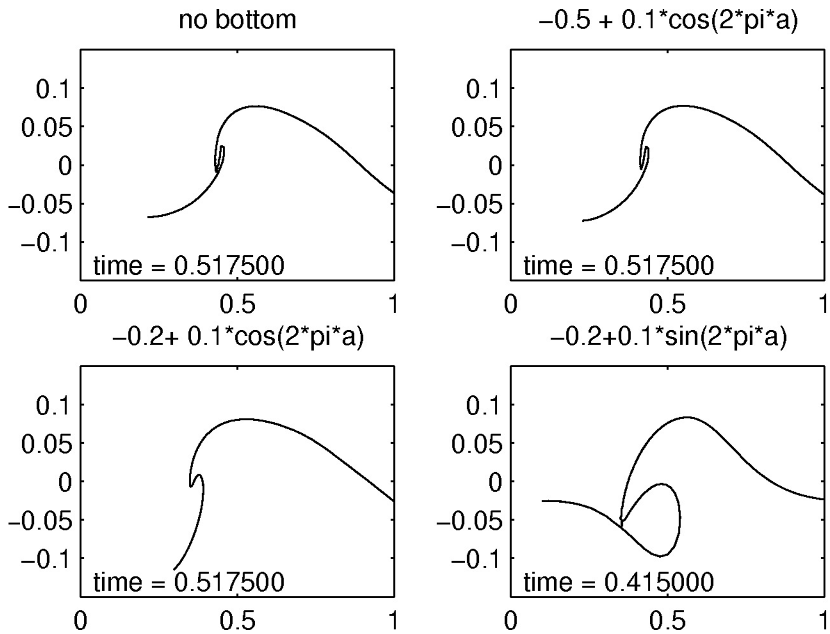

Figure 13 the fourth subgragh blows up first at $t = 0.4150$ then at $t = 0.5175$, the first and second subgragh blow up.

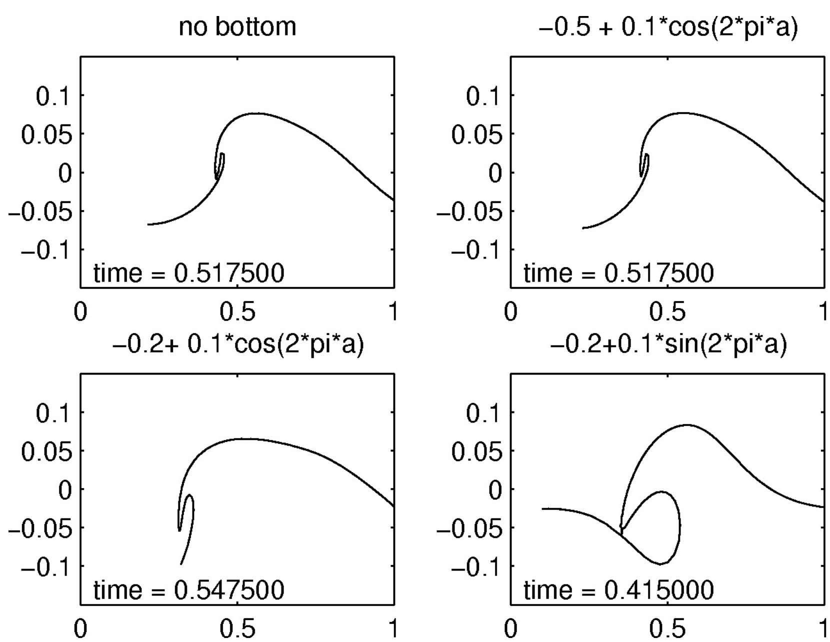

Figure 14 the third subgragh blows up at $t = 0.5475$

It seems that only when the bottom is rather close to the surface, the effect of the bottom is able to be remarkable. Finally we give two examples about breaking wave above rising-step bottom and descending-step bottom. In these case, the bottom is more shallow and the difference is more remarkable. Judging from these two figures , we find that the height of breaker changes with the step and its appearance is far earlier than that in the case of infinite depth.

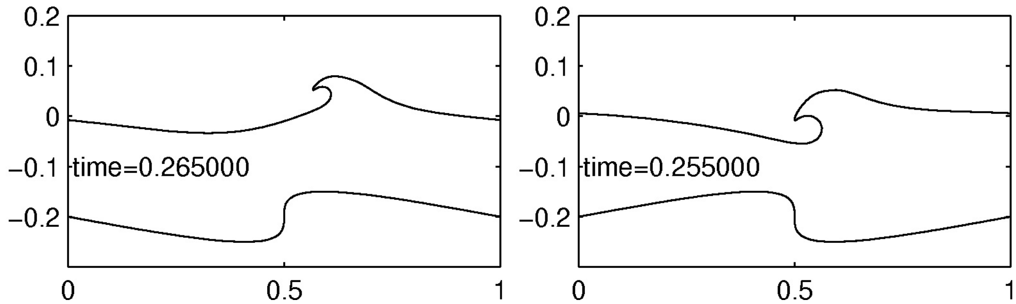

Figure 15

The left bottom topography has the form $(\alpha - sin(2\pi(\alpha-0.5))/(2\pi), -0.2+0.05\sin(2\pi(\alpha-0.5)))$, and the right has the form $(\alpha - sin(2\pi(\alpha-0.5))/(2\pi), -0.2-0.05\sin(2\pi(\alpha-0.5)))$.

Acknowledgement. We would like to acknowledge professor Zhenhuan Teng for a number of interesting discussions during the preparation of this work.

References

[1] Batchelor, G.K., An introduction to Fluid Dynamics, Cambridge University Press, 1994.

[2] Baker, G., Meiron, D., Orszag, S., Generalized vortex methods for free-surface flow problems, *J. Fluid Mech.,* **123** (1982), 477-501.

[3] Baker, G., Nachbin, A., Stable Methods for Vortex Sheet Motion with Surface Tension, 1992.

[4] Beale, J.T., Hou, T.Y., Lowengrub, J.S., Growth rates for the linearized motion of fluid interfaces away from equilibrium, *Comm. on Pure and Applied Math.,* **XLVI** (1993), 1269-1301.

[5] Beale, J.T., Hou, T.Y., Lowengrub, J.S., Convergence of a boundary integral method for water waves, *SIAM J. Numer. Anal.,* **33**:5 (1996), 1797-1843.

[6] Birkhoff, G., Helmholtz and Taylor instability, *Proc. Symp. Appl. Math.,* **13** (1962), 55-76.

[7] Calflisch, R., Orellana, O., Singular solutions and ill-posedness for the evolution of vortex sheets, *SIAM J. Math. Anal.,* **20** (1989), 293-307.

[8] Craig, W., An existence theory for water waves and the Bousinesq and the Korteweg-de Vries scaling limits, *Comm. Partial Diff. Eqns.,* **10** (1985), 787-1003.

[9] Craig, W., Sulen, C., Numerical Simulaiton of gravity waves, *J. Comp. Phys.,* **108** (1993), 73-83.

[10] Dold, J.W., An efficient surface-integral algorithm applied to unsteady gravity waves, *J. Comp. Phys.,* **103**:9 (1992), 90-115.

[11] Dommermuth, D.G., P.Yue, D.K. , A high order spectral method for the study of nonlinear gravity waves, *J. Fluid Mech.,* **184,** (1987), 267-288.

[12] Fenton, J.D., Rienecker, M.M., A fourier mothod for solving nonlinear water-wave problems: application to solitary-wave interactions, *J. Fluid Mech.,* **118** (1982), 411-443.

[13] Glozman, M., Agnon, Y., Stiassnie, M., High-order formulation of the water-wave problem, *Phys. Rev. D.,* **66** (1993), 347-367.

[14] Hou, T., Lowengrub, J., Krasny,R., Convergence of a point vortex mehtod for vortex sheets, *SIAM J. Numer. Anal.,* **28** (1991), 308-320.

[15] Hou, T., Lowengrub, J., Shelley, M., Removing the stiffness from interfacial flows with surface tension, *J. Comp. Phys.,* **114** (1994), 312-338.

[16] Hou, T., Zhang P., A new Stablizing Technique for Boundary Integral Methods, *Math. Comp.,* **70**:235 (2001), 951-976.

[17] Kenig, C.E., Recent progress on boundary value problems on Lipschitz domains, *Proc. Symp. Pure Math.,* **53** (1985), 175-205.

[18] Kenig, C.E., Elliptic boundary value problems on Lipschitz domains, *Ann. Math. Studies,* **112** (1986), 131-183.

[19] Kerr, R.M., Simulation of Rayleigh-Taylor flows using vortex blobs, *J. Comp. Phys.,* **76** (1988), 48-84.

[20] Krasny, R., Desingularization of periodic vortex sheet roll-up, *J. Comp. Phys.,* **65** (1986), 292-313.

[21] Longuet-Higgins, M.S., Cokelet, E.D., The deformation of steep surface waves on water,I. a numerical method of computation, *Proc. Rev. Soc. London Ser. A.,* **350** (1976), 1-26.

[22] Moore. D.W., On the point vortex method, *SIAM J. Sci. Statist. Comp.,* **2** (1981), 65-84.

[23] Moore. D.W., Groffith-Jones, R., The stability of an expanding circular vortex sheet, *Mathematika,* **21** (1974), 128-133.

[24] New, A.L., Mclver, P., Peregrine, D.H., Computations of overturning waves, *J. Fluid Mech.,* **150** (1985), 233-251.

[25] Peregrin D.H., Breaking waves on beaches, *Ann. Rev. Fluid Mech.,* **15** (1983), 149-178.

[26] Pullin, D.J., Numerical studies of surface-tension effects in nonlinear Kelvin-Helmholtz and Rayleigh-Taylor instability, *J. Fluid Mech.,* **119** (1982), 507-532.

[27] Roberts, A.J., A stable and accurate numerical method to calculate the motion of a sharp interface between fluis, *J. Appl. Math.,* **31** (1983), 13-35.

[28] Sharp, D.L., An overview of Rayleigh-Taylor instability, *Physica D,* **12** (1984), 3-18.

[29] Schwartz, L.W., Fenton, J.D., Strongly nonlinear waves, *Ann. Rev. Fluid Mech.,* **14** 91982), 39-60.

[30] Shelley, M.J., A study of singularity formation in vortex sheet motion by a spectrally accurate method, *J. Fluid Mech,* **244** (1992), 493-526.

[31] Sidi. A., Israeli, M. Quadrature methods for period singular and weakly singular Fredholm integral equations, *J. Sci. Comp.,* **3** (1984), 47-67.

[32] Tryggvason, G., Numerical simulations of the Rayleigh-Taylor instability, *J. Comp. Phys.,* **75** (1988), 253-282.

[33] Vinje, T., Brevig, P. Numerical simulation of breakng waves, *Adv. Water Resources,* **4** (1981), 77-82.

[34] Verchota, G.C., Layer potentials and regularity for the Dirichlet problem for Laplace's equation in Lipschitz domains, *J. Func. Anal.,* **59** (1984), 572-611.

[35] Yeung, R.W., Numerical methods in free-surface flows, *Ann. Rev. Fluid. mech.,* **14** (1982), 395-442.

[36] Yosihara, H. Gravity waves on the free surface of an incompressible perfect fluid of infinit depth, *RIMS Kyoto,* **18** (1982), 49-96.